

CHAPTER 5

MECHANICAL PERFORMANCE OF STRUCTURAL EPOXY ADHESIVE EXPOSED TO TROPICAL CONDITIONS

5.1 Introduction

A brittle material is one which exhibits relatively small extensions to fracture resulting in the partially plastic region of the tensile test graph to be much reduced. In the overview of brittle materials, mechanical behaviour is determined by stress and strain associated with material points throughout the material. Mechanical properties are measured in test of samples in which loads or boundary displacements are applied in such way that the relation between stress and strain at a typical point can be inferred. In brittle materials, the situation is further complicated by the occurrence of fracture. During deformation, the material structure changes due to the initiation and propagation of cracks at different locations throughout the material [87]. Problems encountered conducting the test for brittle materials include devising specimen and loading configuration in order to produce a state of uniform plane stress. The problem increases significantly with the application of brittle composite materials and brittle adhesives system nowadays in mechanical and civil engineering applications.

The shear properties of epoxy adhesive is one aspect that the user tends to neglect as it is only a small part, but it is crucial in designing the externally bonded FRP to reinforced concrete members. The selection of adhesive is important to provide sufficient material integrity in order to produce uniform stress throughout the bond area. This is necessary to avoid the premature failure such as adherend failure, cleavage and interfacial failure of adhesive. In general, the typical shear test method used to determine the shear properties of most materials is the cylinder-torsion test method. The method is able to determine the shear properties by analysing stress elements at various angles or distances from cylindrical section centre as shown in Fig. 5.1. Unfortunately, this method has a weakness that it is unable to produce a significant section on the specimen, and the grips strongly influence the state of stress.

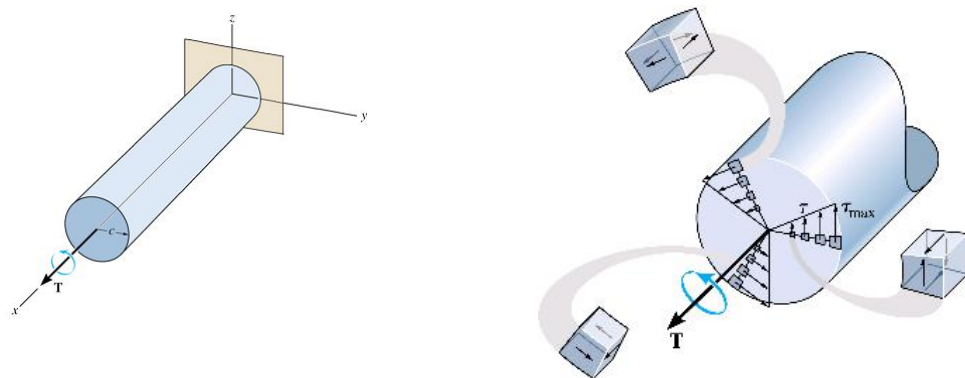


Fig. 5.1: The concept of cylinder torsion test method [88]

In 1978, Arcan *et al.* [62] introduced a new method of testing material shear properties under uniform plane stress conditions by means of a specially designed plane specimen, as shown in Fig. 2.41 (Chapter 2). The fixture was used to determine shear properties for various materials such as polymer composite, sandwich materials system, human bones and solid polymers. Photoelasticity analysis had shown that in the significant section of the specimen it was possible to produce a uniform plane stress with high degree of accuracy. The compact nature of the Arcan fixture offered an advantage to obtain the shear properties in all in-plane directions in a relatively simple manner. The Arcan fixture was used to produce both shear and axial forces to the test specimen and this special case of loading produced pure shear on the

significant section and the experimental results were encouraging and acceptable with high degree of confidence [62].

5.2 Study Objective

The main objective of this experimentation was to study the in-plane shear properties of brittle structural epoxy material exposed to tropical environmental conditions using Arcan Test Method.

5.3 Scope of study

The scope of this study covered the following topics;

- i. Literature study on the epoxy adhesive material (as discussed in Chapter 2);
- ii. Literature study on the Arcan test method (as discussed in Chapter 2);
- iii. Specimen preparation;
- iv. Specimen experimentation, load test and microstructure analysis;
- v. Results and discussions;
- vi. Conclusions.

5.4 Methodology

The literature studies were carried out by sourcing the related information from journals, handbooks, books, previous theses, and websites. Firstly, literature review was carried out to understand the mechanical characteristic of the adhesive system used in this study. Then, the studies focused on the Arcan test method in order to investigate the theoretical background related to shear properties and to determine a suitable butterfly specimen geometry for the study. Apart from that, a

study on Arcan test rig development has also been conducted in order to identify the problems faced by previous researchers.

The two parts epoxy adhesive was cast in a closed metal mould to produce butterfly shaped specimens. The specimens were exposed to four conditions that represented tropical environments, namely; Laboratory (ESLT-LB), Outdoor (ESLT-OD), Plain Water (ESLT-PW: wet/dry) and Salt Water (ESLT-SW: wet/dry). The salt water and plain water specimens were exposed to their respective conditions for 7 days wet followed by 7 days dry for 24 cycles in total. All the specimens were exposed for six months period. After the completion of experimentation works, the specimens were sent to materials testing laboratory for a final load test up to failure. The shear test was carried out by using Instron Universal Testing Machine Series IX Model 4206 that was equipped with Arcan test fixture. The fracture surface of the test specimens for each exposure condition was then sent to material laboratory for microstructure analysis.

Data were gathered from the instrumented measurement that was established during testing. The specimen failure mechanism was observed during testing and microstructure analysis was done in order to investigate in depth the source of failure mechanism. The experimental results were discussed and compared with previous research findings.

5.5 Specimen Preparation

In this section, the discussion focuses on the test specimen preparation which includes the material details, specimen geometry, casting process and polishing. The final geometry measurements, quality checks and marking are described in detail.

5.5.1 Material Details

The epoxy namely Selfix Carbofibe adhesive, supplied by Exchem, United Kingdom was used. The properties of Selfix Carbofibe adhesive were achieved by blending/mixing a modified epoxy resin and inorganic fillers to form a base component, which was activated by a thixotropic formulated amine hardener. The mixture was very viscous and light grey (almost white) in colour. The epoxy system was difficult to mould due to its high viscosity and it took about 24 hours to reach curing stage. The curing time was subjected to ambient laboratory condition. This epoxy adhesive consisted of two parts, namely; part A and part B (Fig 5.2). Both parts were mixed with a ratio of 3:1 as stated in the supplier's specification. Their chemical formulations and cast properties are listed as in Table 5.1 and Table 5.2.

Table 5.1: Chemical formulation of Selfix Carbofibe epoxy adhesive [35]

Materials	Chemical formulation	Colour
Part A (Epoxy)	Contains 35 to 45% reaction product of Epichorohydrin Bisphenol A epoxide resin of average molecular weight < 700	White
Part B (Hardener)	Contains 3,6,9,12-tetra-azatetradecamethylenediamine (< 20%) and 4,4-isopropylidenediphenol (< 10%)	Dark Grey

Table 5.2: Typical mechanical and physical properties of Selfix Carbofibe epoxy adhesive [35]

Property	Value
Compressive strength (MPa) aged of 7 days at 20 °C	90
Tensile strength (MPa)	23
Thermal expansion /°C	33×10^{-6}
Tensile modulus (GPa)	10
Shear modulus (GPa)	na
Single lap shear strength (MPa)	> 18
Glass transition temperature (DMTA) °C	> 65
Water absorption	0.4%



(a)

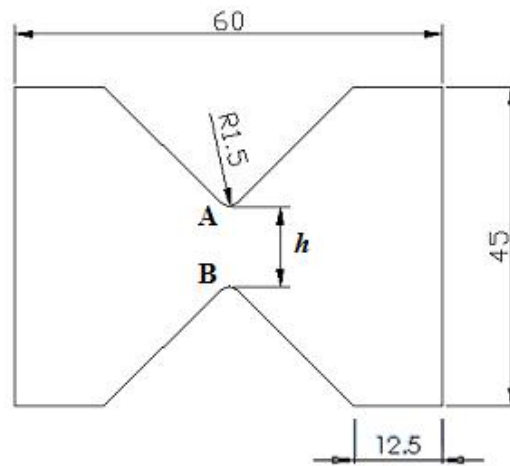


(b)

Fig. 5.2: Two parts of Selfix Carbofibe adhesive (a) Part A (b) Part B

5.5.2 Specimen Geometry

The specimen size of 60 mm long \times 45 mm wide with an average thickness of 4.4 mm was used for the experimentation study as shown in Fig. 5.3. The 90° notches were formed at the centre of 60 mm length (at the top and bottom) such that the distance between notches was left about 10 mm at the middle to introduce shear field on the significant section, AB. A notch radius of 1.5 mm was produced to minimise stress concentration and also to produce a uniform shear stress distribution along the significant section [65].



* All dimensions in mm

Fig. 5.3: The butterfly specimen geometry

5.5.3 Specimen Casting Process

The butterfly shaped cast epoxy specimens were prepared by mixing two parts of adhesive system consisting of epoxy and hardener with the ratio of 3:1. Butterfly shape specimens were produced by casting the mixture into a female mould. To produce five (5) pieces of butterfly shaped specimens, 5 sets of the mixture (i.e. total weight of 210 gram epoxy and 70 gram hardener) were prepared as shown in Fig. 5.4.

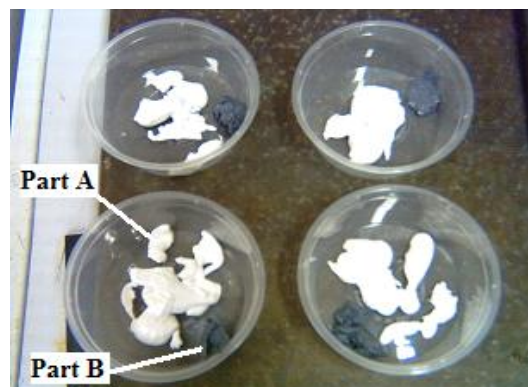


Fig. 5.4: Adhesive compositions: Epoxy (Part A – white) and Hardener (Part B - dark grey)

A low speed electric mixer was used to mix the materials until the mixture turned soft grey in colour, which means that the colour of the mixture turned from white and dark grey to soft grey colour, as shown in Fig. 5.5. Due to its short pot life, the mixture was mixed in small quantities in plastic containers. The mixing process was done in the laboratory control room where the temperature and relative humidity was in the range of 24 to 26°C and 40 to 55% (i.e. by depending on the ambient laboratory condition).



Fig 5.5: A mixing process using electric mixer

The butterfly shaped specimens were cast by using mild steel moulds which consisted of male parts (top) and female parts (base). The mould surfaces were cleaned by using a soft cloth and Carnauba wax to ensure that they were free from dirt and dust before being used for casting. This mould parts cleaning process is shown in Fig. 5.6. After the cleaning process, two flat plates were attached to cover the back part of the mould by screws as shown in Fig. 5.7 (a) and (b). The casting process started by filling the epoxy into the female part mould. The process was carefully done by using a metal scraper to ensure minimum air entrapment in the mixture (Fig. 5.8).



Fig. 5.6: Cleaning the mould using soft cloth with Carnauba wax



(a)



(b)

Fig 5.7: Flat plate attached to male part by screws (a) Flat plate before installation and (b) Flat plate after installation



Fig. 5.8: Filling the epoxy mixture into the mould cavity

The male mould part was then attached to the female part, which means to form a solid butterfly shape as shown in Fig 5.9. A metal block weight of about 10 kg was placed onto the top of the mould to produce an extra uniform pressure on the

mould as shown in Fig 5.10. Finally the specimens were left in a laboratory environment with temperature ranging from 23 to 33°C for at least 24 hours for full chemical reaction (i.e. curing) prior to demoulding.



Fig. 5.9: Male part attached to the female part



Fig. 5.10: A weight used to press the female part from top side

Demoulding process of the specimens was carefully done by applying a soft knocking force onto the butterfly shaped Teflon block using a wood hammer (Fig. 5.11). After demoulding, the specimens were brought to the materials laboratory for the polishing process. This process was done by using Mecapol P255 U Polish Machine to make the surfaces of the specimen smoother and the sharp edges rounder. The process is shown in Fig. 5.12 (a) and (b).



Fig. 5.11: Specimen demoulding using Teflon block and wood hammer



(a)



(b)

Fig. 5.12: Surface grinding and polishing (a) Mecapol P255 U polishing machine (b) Manual polishing technique

In the final stage prior to the exposure to the designated conditions, the specimens were checked on their quality, established their code name and date of manufacture, as shown in Fig. 5.13. All specimens were conditioned in room environment with a temperature ranging from 25 to 33°C and relative humidity of 70 to 90% for 7 to 14 days before to ensure the specimens were fully cured. Five specimens for each group of samples were selected for the experimentation study programme.



Fig. 5.13: Specimens ready to be exposed

The recorded data showed that the average specimen width, thickness and cross sectional area were in the range of 10.94 to 11.20 mm, 4.35 to 4.51 mm and 48.73 to 49.44 mm² respectively, as shown in Table 5.3.

Table 5.3: Butterfly specimen's width, thickness and significant area average measurement

Sample Code	Width (mm)	Thickness (mm)	Significant area (mm ²)
ESST-CO	10.94	4.46	48.78
ESLT-LB	10.96	4.51	49.44
ESLT-OD	11.20	4.35	48.73
ESLT-PW	10.98	4.46	49.03
ESLT-SW	11.05	4.47	49.41

5.6 Selfix Carbofibe Adhesive Durability Experimentation Programme

The specimens were exposed to four different types of environmental conditions that reflected the tropical climatic conditions, namely; laboratory condition (LB), outdoor condition (OD), and exposure to plain and salt water under wet/dry cycles. The wet and dry cycles were 7 days wetting and 7 days drying, respectively, and was conducted in two separate controlled laboratory rooms, i.e. one for plain water and the other for salt water condition.

5.6.1 Environmental Exposure Conditions

The test matrix of environmental durability exposure conditions designed for this research programme is given in Table 5.4. The number of test specimens per sample for each candidate condition and their number of cycles are clearly indicated. The individual effects of each exposure condition were evaluated. In this programme, climatic tropical exposures which include: laboratory condition, plain water wet/dry cycle resistance, salt water wet/dry cycle resistance and weathering (natural) resistance were established.

Table 5.4: The Selfix Carbofibe epoxy adhesive experimentation programme

Sample code/Exposure conditions	Laboratory	Outdoor	Salt water (wet/dry)	Plain water (wet/dry)
ESST (control)	5S			
ESLT (exposed)	5S	5S	5S (24 cycles) Exposure for 6 months 1 week/cycle	5S (24 cycles) Exposure for 6 months 1 week/cycle

Note: 5S represent five specimens per group of sample

For the laboratory (LB) exposure condition, the specimens were exposed to a condition of 75 to 90% of relative humidity (RH) and 23 to 33°C of room temperature. The specimens were placed on aluminium angle bars supported by mild steel rack and held in a horizontal position. The specimens' exposed surfaces were rotated weekly. Plain water and salt water was selected to study the effects of prolonged immersion of specimens in tropical climate and ocean tropical water. Normal plain (tap) water was used for water resistance exposure condition.

Substitute ocean tropical water was prepared following the standard manufacturer's specification (i.e. tropical ocean salt for aquarium was used for the salt water resistance exposure). Immersion of specimens in plain water and salt water was done by using 50 litres capacity of GFRP cylindrical tanks. The important water quality parameters and environmental conditions can be referred to in Table 4.5, Table 4.7 and Table 4.8 (section 4.6.1: Chapter 4).

The specimen preparation process for each conditions of exposure is shown in Fig. 5.14 (a) to (f). Firstly, the GFRP cylindrical tanks were filled with plain (tap) water and salt by 1: 27.5 ratio (i.e. 1 litre of plain water added with 27.5 gram of tropical ocean salt). For an outdoor exposure conditions the specimens were placed on aluminium bars. The specimens' surfaces were alternately rotated (weekly). At the end of the exposure period, the specimens were brought in to the laboratory to prepare for final load test within two weeks time.



Fig. 5.14 (a): Adding salt in plain water



Fig. 5.14 (b): Salt water mixing process



Fig. 5.14 (c): Specimens in plain water condition



Fig. 5.14 (d): Specimens in salt water condition



Fig. 5.14 (e): Specimens in control room condition

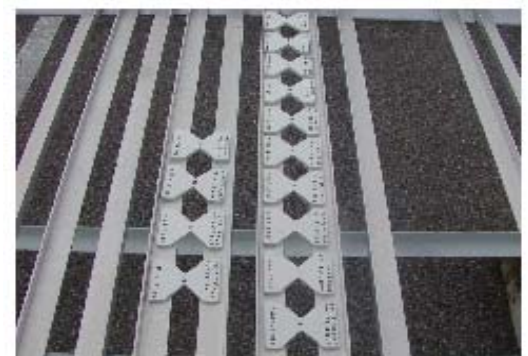


Fig. 5.14 (f): Specimens exposed to outdoor condition

5.7 Instrumentation, Measurement and Testing

In the following sub-sections, the details of strain gauge installation, fixing procedure of Arcan test fixtures, load test set-up and specimen's microstructure analysis using Field Emission Scanning Electron Microscope (FESEM) were discussed.

5.7.1 Strain Gauge Installation

A rosette type strain gauge, TML FCA-1-11 with 1 mm gauge length was installed onto the butterfly specimen at the centre of the significant area AB (Fig. 5.15). The gauge was installed in the direction of $\pm 45^\circ$ measured from the specimen's horizontal axis. Before installation, the gauge bond surface in the significant area was prepared (roughened) with 1000 grade grain size sand paper prior to cleaning by using liquid acetone to remove grease, dust or dirt. Then, the strain gauge was attached onto the specimen by referring to standard installation procedure. The complete gauge attachment onto the butterfly specimen is shown in Fig. 5.16 and the important parameters of the gauge specification are shown in Table 5.5.

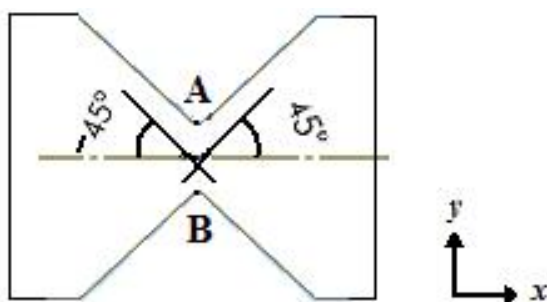


Fig. 5.15: Rosette type strain gauge installation direction

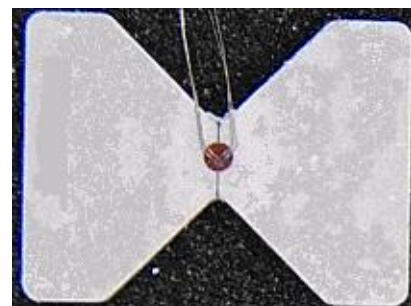
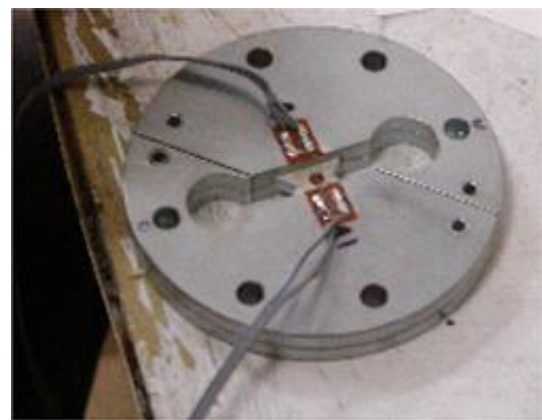


Fig. 5.16: Complete gauge installation onto the butterfly specimen

Table 5.5: TML FCA-1-11 Rosette strain gauge specifications [81]

Manufacturer	Tokyo Sokki Kenkyujo Co. Ltd. Japan
Gauge type	TML FCA-1-11
Gauge factor	1 = 2.08, 2 = 2.08 \pm 1%
Coefficient of thermal expansion	11.8 x 10 ⁻⁶ /°C
Tolerance	\pm 0.85 (μ m/m)/°C
Temperature coefficient of gauge factor	+ 0.1 \pm 0.05%/10°C

After the specimen was completely installed with the strain gauge, adhesive film thickness of 0.1 mm was bonded onto both male and female Arcan fixtures (grips) to ensure that the butterfly specimen was perfectly fixed in order to prevent it from slipping during loading. Then the male grip was used to clamp the butterfly specimen and four screws were used to tighten them together at the upper side and the lower side diagonally. These screws were carefully tightened to make sure that the specimen plane surface did not experience stress. The soldering technique was used to join the strain gauge lead wire to the terminal (i.e. previously bonded onto the Arcan fixture). The process was carefully handled in order to prevent the terminals from being disconnected (over tensioned) during loading. The gauge installation preparation is shown in Fig. 5.17 (a) to (c).

**Fig. 5.17 (a):** Arcan male grip attached onto female grip**Fig. 5.17 (b):** Complete assembly of butterfly specimen

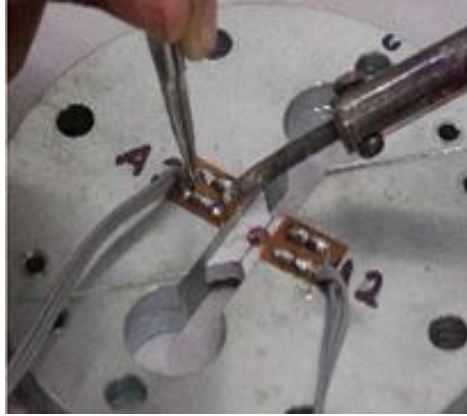


Fig. 5.17 (c): Soldering lead wire to terminal

5.7.2 Arcan Test Fixture Set-Up

The modified Arcan test fixture used in this study programme consisted of a pair of male and female parts, as shown in Fig. 5.18. The exact shape and size of specimen was mounted into the female part followed by the male part. Both parts were tightened by screws to ensure that the specimen was tightly gripped between the fixtures to prevent from slippage and misalignment during loading. The complete assembly of the fixtures was attached to the holder at the lower and upper parts accordingly prior to attachment to the Instron Universal Testing Machine, as shown in Fig. 5.19. The tensile loads were applied on the Arcan fixture through holders before the loading configuration was changed to shear mode that was finally imposed on the specimen. The direction of principal shear then acted in the direction of $\pm 45^\circ$ as referred to the specimen horizontal axis.

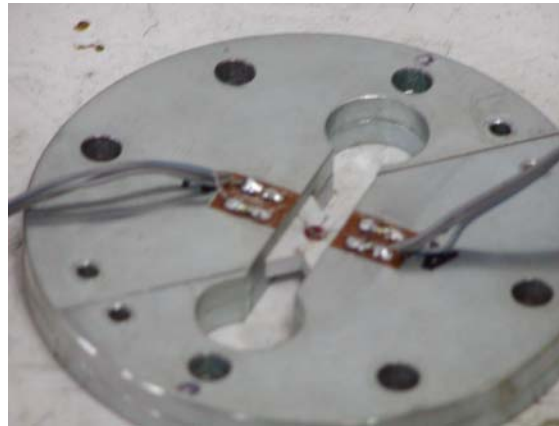


Fig. 5.18: Arcan fixture assembly

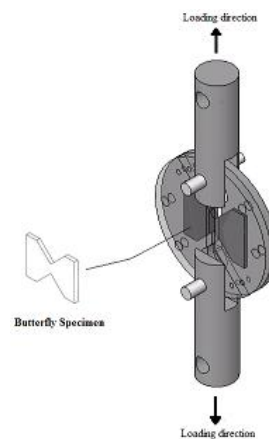


Fig. 5.19: Assembly drawing of Arcan fixture set-up

The fixture holders were attached to the loading machine, namely Universal Testing Machine by two pins with a diameter of 15 mm as shown in Fig. 5.20 (a). After the holders were attached to the loading machine, the complete Arcan grip fixture consisting of the butterfly specimen was connected to the holders by using two pins at the upper and lower sections of the Arcan plate. All the pins were carefully checked to ensure that the connection was in perfect adjustment before applying the load, as shown in Fig. 5.20 (b).



Fig. 5.20 (a): Attachment grip to holder by pin

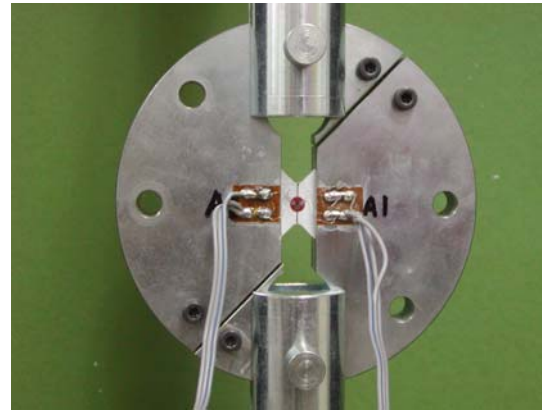


Fig. 5.20 (b): Complete Arcan fixture attachment to holder

The complete instrumentation and measurement system is shown in Fig. 5.21. It was equipped with the following important features;

- i. A load frame where the Arcan fixture was installed and loaded in tensile
- ii. A control panel that controlled the testing parameters such as loading rate
- iii. A computer for the user to key-in the information and the properties of the specimen and set the format for the plotting of graphs and results
- iv. A data logger to record and print out the strain readings

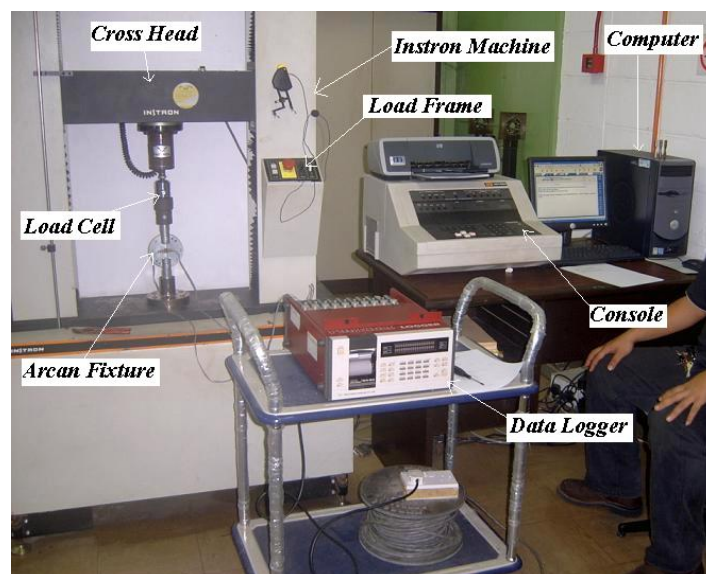


Fig. 5.21: Instrumentation set-up for Arcan Test

5.7.3 Testing Procedure

The Arcan fixture equipped with butterfly specimen was loaded in tension by using Instron Universal Testing Machine Series IX Model 4206 instrumented with 5 kN load cell. The loading rate was set-up to 1 mm/min and the specimen was loaded up to failure. The specimen principal strains ($\pm 45^\circ$) were measured at every 0.1 kN load increment and this was manually recorded by TDS 302 data logger until near to failure. The applied load and machine displacement were recorded automatically by the computer. Apart from that, a stop watch was used to measure the time to failure for each specimen. As a result, the relationship between the applied shear stress and shear strain could be established by dividing the applied load on the cross-sectional area of the significant section. The testing process is shown in Fig. 5.22 (a) to (c).



Fig. 5.22 (a): Completion set-up of Arcan fixture to the loading machine



Fig. 5.22 (b): Initializing strain reading



Fig. 5.22 (c): Recording test data

5.7.4 Field Emission Scanning Electron Microscope (FESEM)

After the test, the surface fracture and microstructure analysis of each sample was done by using Field Emission Scanning Electron Microscope (FESEM). FESEM is a microscope that works with electrons (particles with a negative charge) instead of light. These electrons are liberated by a field emission source. The object is scanned by electrons according to a zig-zag pattern. Electrons are liberated from a field emission source and accelerated in a high electrical field gradient. Within the high vacuum column these so-called primary electrons are focused and deflected by electronic lenses to produce a narrow scan beam that bombards the object. As a result secondary electrons are emitted from each spot on the object. The angle and velocity of these secondary electrons relates to the surface structure of the object. A detector catches the secondary electrons and produces an electronic signal. This signal is amplified and transformed to a video scan-image that can be seen through monitor or through digital image and processed for further analysis. FESEM was used in this project to visualize very small topographic details on the surface of fractured objects and also to determine the elemental composition measurement of each sample. The FESEM machine shown in Fig. 5.23 consists of five important features that are listed in Table 5.6.

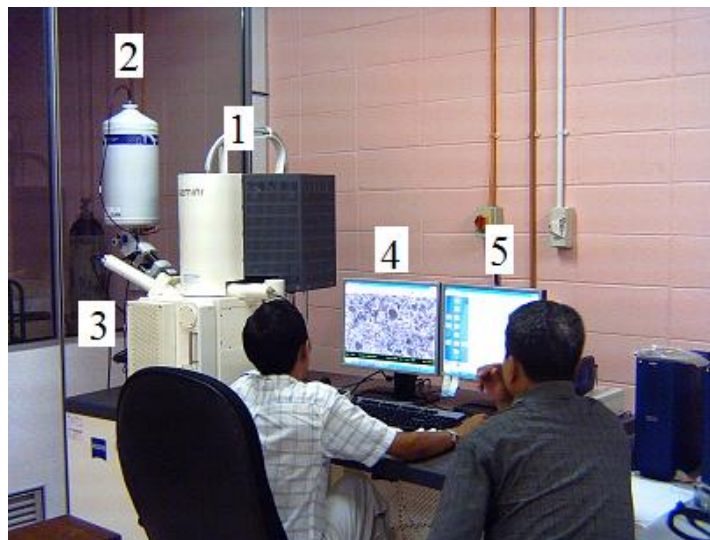


Fig. 5.23: Field-emission Scanning Electron Microscope (FESEM)

Table 5.6: FESEM machine main features

No.	Feature	Function
1	Cryo Unit	A cylindrical column that is mounted on a desk and used to host the electron beam.
2	Liquid Nitrogen Container	To maintain the vacuum and the temperature in the instrument and the Cryo unit.
3	Vacuum Chamber Unit	A small chamber where the specimens are installed, washed and dried to produce fine structures.
4	Control Panel	To control and manipulate the object through large screen.
5	Second Control Panel	A small screen to watch the object in chamber during scanning.

5.8 Results and Discussion

The results and discussion focus on the experimental data analysis for control and exposures test specimens. The determination of shear properties of Selfix Carbofibe adhesive specimen due to tropical exposure conditions through Arcan method was the main parameter discussed. The results were analysed and presented in terms of graphs and tables to provide a more comprehensive technical discussion. Overall, the discussion was referred to a selected significant specimen from each group of test samples and finally, the conclusion focused on the average performance results of these sample groups. The overall discussion also covered the microstructure analysis that was performed on the surface and cross-section of fracture parts of the specimens. This was to support the analytical test data that was previously discussed.

5.8.1 Test Rig-Specimen Evaluation

The evaluation on the test rig-specimen reliability was done through the construction of Mohr circle and graph of shear strain versus shear stress for each respective candidate specimen.

From load test, it could be observed that all specimens failed in brittle form. The fracture line occurred at about 45° angle measured from the specimen principal axis to the gauge length vertical line. This confirmed that the specimens failed in the direction of principal stresses (i.e. failure characteristic of brittle material). This was consistent with the theoretical analysis, where the direction of principal stresses is at 45° from pure shear stress plane (gauge section). By visual inspection on the fractured part, it could be seen that the specimen failure occurred almost perfectly at 45° angle.

The applied load, strain, time to failure and mode of failure were recorded and observed for every single specimen. However, the properties such as shear stress, average shear strength, average shear strain, and shear modulus were determined through equations [5.1] to [5.3].

i. Shear stress, τ_{xy}

$$\tau_{xy} = P / (b_s \times h_s) \text{ (N/mm}^2\text{)} \quad [5.1]$$

where,

P = load (N)

b_s = length of significant section (mm)

h_s = thickness of significant section (mm)

ii. Shear strain, γ_{xy}

$$\gamma_{xy} = 2(\epsilon_x)_{\theta=45^\circ} \quad [5.2]$$

where

$(\epsilon_x)_{\theta=45^\circ}$ = strain at 45° with respect to specimen horizontal axis x

iii. Shear modulus, G_a

$$G_a = \Delta\tau / \Delta\gamma \text{ (kN/mm}^2\text{)} \quad [5.3]$$

where

$\Delta\tau / \Delta\gamma$ = slope of the plot of shear stress as a function of shear strain within the linear portion of the curve

The principal strain data in the directions of -45° and $+45^\circ$ were used to calculate the shear strain. By using equation [5.1] and [5.2], the shear stress-strain relations for each gauge specimen could be obtained. This was done by subtracting the strain in the -45° direction from the $+45^\circ$ direction. As a result, the shear stress-strain relations for each gauge specimen were obtained. The elastic shear modulus was then determined using the least square fit (i.e. curve gradient) of the earlier stage of the shear stress-strain curve.

Finally, in order to evaluate the alignment of specimen stress element, the following calculation was done by assuming that the shear stress distribution along the specimen significant section, AB was uniform. A sample calculation was done for specimen ESLT-LB01 as follows;

Specimen thickness, $t = 4.43$ mm

Specimen significant gauge length, $h = 10.93$ mm

Load carried by the specimen at load, $F = 1000$ N

Principal strain in $+45^\circ$ direction, $\varepsilon_{45^\circ} = 4112 \mu\varepsilon$

Principal strain in -45° direction, $\varepsilon_{-45^\circ} = -3646 \mu\varepsilon$

The average shear stress, τ_{ave} and shear strain, γ can be determined as follows;

$$\begin{aligned} \text{Specimen cross sectional area, } A_o &= t \times h \text{ mm}^2 \\ &= \underline{\underline{48.42 \text{ mm}^2}} \end{aligned}$$

From equation (3.4), the average shear stress, τ_{ave} is;

$$\begin{aligned} \tau_{ave} &= \frac{F}{A_o} \\ \tau_{ave} &= \frac{1000}{49.21 \times 10^{-6}} \\ &= \underline{\underline{20.32 \text{ MPa}}} \end{aligned}$$

and, from equation (3.5), the shear strain, γ is;

$$\begin{aligned}\gamma &= \varepsilon_{+45^\circ} - \varepsilon_{-45^\circ} \\ &= (4112) - (-3646) \\ &= \underline{\underline{7758 \mu\varepsilon}}\end{aligned}$$

Therefore, the alignment of the stress element can be determined from the following equation and finally, the state of strains of the stress element can be produced from a Mohr's circle construction based on the above strains values as shown in Fig. 5.24.

$$\begin{aligned}\varepsilon_{ave} &= \frac{\varepsilon_{45^\circ} + \varepsilon_{-45^\circ}}{2} \\ \varepsilon_{ave} &= \frac{4112 - 3646}{2} \\ \varepsilon_{ave} &= \underline{\underline{233 \mu\varepsilon}}\end{aligned}$$

$$\begin{aligned}\text{Centre of circle, } C = \varepsilon_x &= \frac{\varepsilon_{45^\circ} + \varepsilon_{-45^\circ}}{2} \\ &= \underline{\underline{233 \mu\varepsilon}}\end{aligned}$$

$$\begin{aligned}\text{Radius of circle, } R &= \frac{\gamma}{2} = \frac{7758 \mu\varepsilon}{2} \\ &= \underline{\underline{3879 \mu\varepsilon}}\end{aligned}$$

$$\text{Diameter of circle, } \phi = 2R = \underline{\underline{7758 \mu\varepsilon}}$$

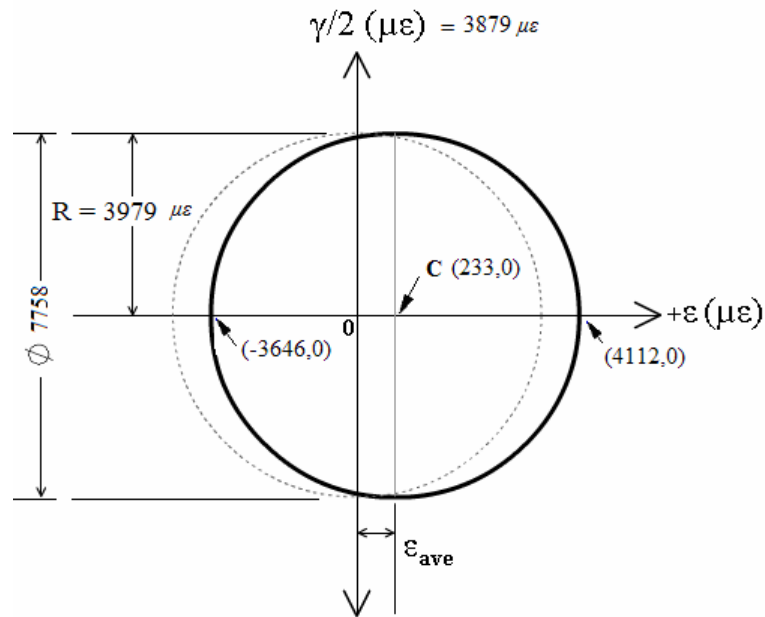


Fig. 5.24: Mohr's circle constructed based on principal strains of ESLT-LB01 at 1000 N load case

From the Mohr's circle shown it can be seen that the pure shear condition did not occur exactly at the mid-section of the specimen where the principal strain was zero. Instead, the pure shear location was slightly shifted to the right of circle centre point. However, this result was still acceptable as the shifting was about 8.5% from the circle radius. On the other hand, practically it was almost impossible to obtain zero error in experiments compared to theoretical analysis. Therefore, the Arcan testing method which was used to determine the shear properties of brittle epoxy specimens could be considered as reliable and justified.

The result showed that the shifting of the stress element as indicated by the average strain value increased as the loading increased. This was due to the nature of brittle materials, where the micro cracks typically propagated rapidly through the specimen as the loading increased. However, the misalignment of the pure shear area was still less than 9% [77]. The result obtained was probably influenced by the non-uniformity of the prepared specimen due to casting process.

From the test results, the overall rig-specimen performances could also be evaluated through graphs of shear strain versus shear stress. The graph was plotted to determine the agreement between the applied stress and strains for both $+45^\circ$ and $-$

45° due to the accuracy of both rig and specimen under load. From the plotted graphs for each candidate test sample specimen, the curve was linearly propagated and about symmetry to the horizontal axis. The average strain difference between both strain directions was about 7% and has not significantly affected the overall results discussions as shown in Fig. 5.25 (a) to (e).

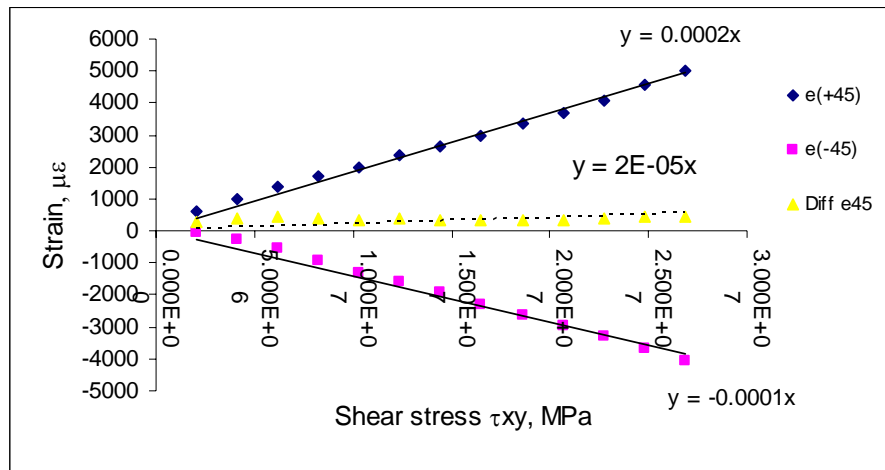


Fig. 5.25 (a): Shear strain versus shear stress for ESST-CO01

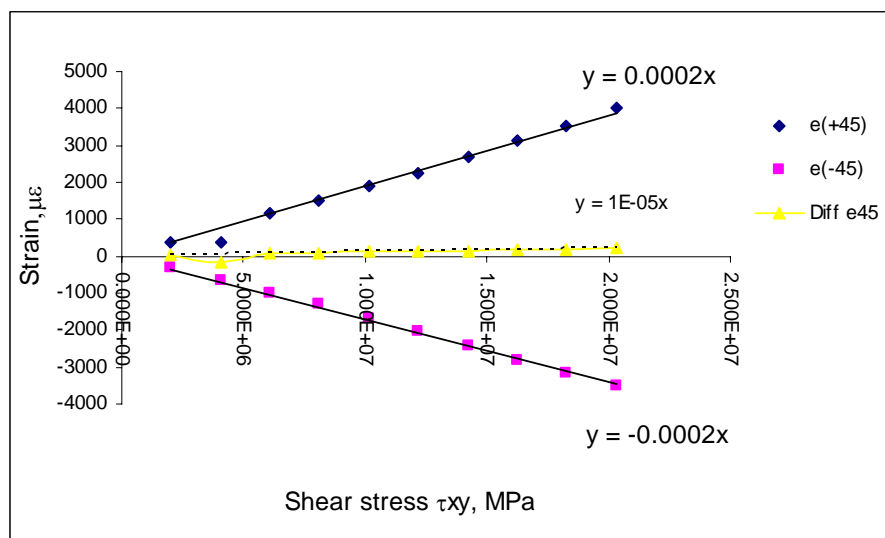


Fig. 5.25 (b): Shear strain versus shear stress for ESLT-LB01

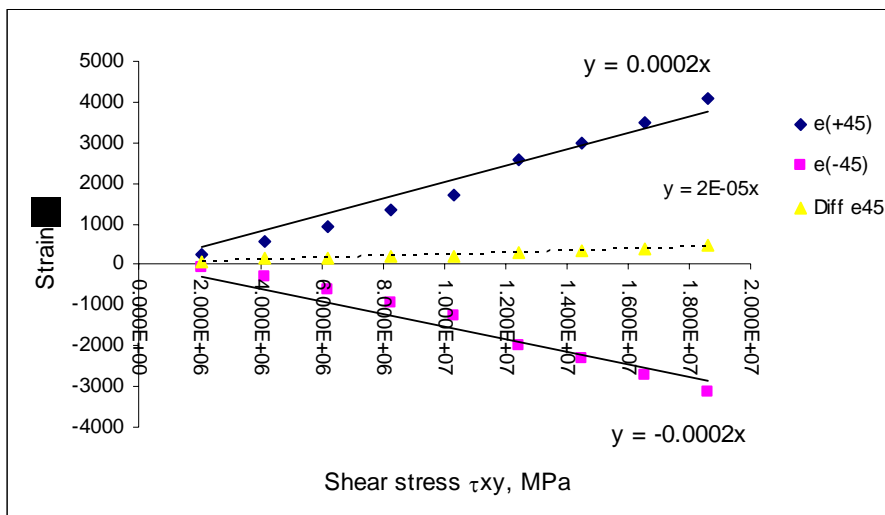


Fig. 5.25 (c): Shear strain versus shear stress for ESLT-OD01

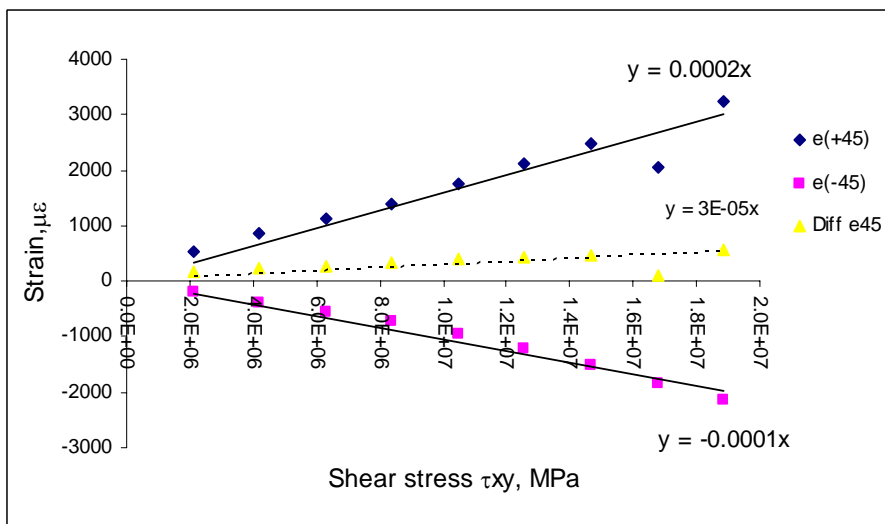


Fig. 5.25 (d): Shear strain versus shear stress for ESLT-PW01

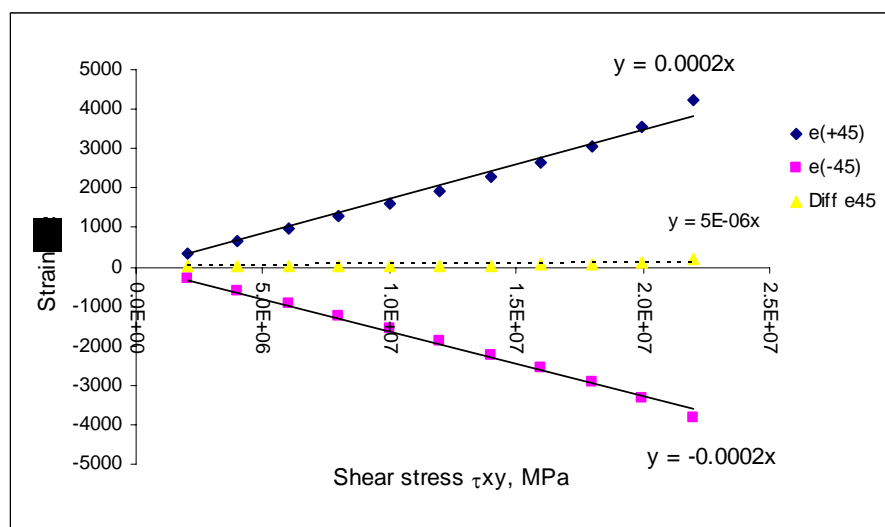


Fig. 5.25 (e): Shear strain versus shear stress for ESLT-SW01

5.8.2 Experimental Results for Control Specimens (ESST-CO)

There were five (5) specimens for the controlled samples. All specimens, ESST-C01 to ESST-C05 have shown brittle characteristics of failure, which occurred at 45° from the specimen's principal axis. The raw data for ESST-C01 specimen are shown in Table 5.7, and the complete test data for the controlled sample, which was calculated from previously stated equations, are shown in Table 5.8.

Table 5.7: Experimental data for ESST-C01

Load (N)	Principal strain ε_{+45} ($\mu\varepsilon$)	Principal strain ε_{-45} ($\mu\varepsilon$)	Average shear stress τ_{ave} (MPa)	Average strain, ε_x ($\mu\varepsilon$)	Shear strain, γ ($\mu\varepsilon$)
100	316	-305	1.84	6	621
200	550	-538	3.69	6	1088
300	945	-939	5.53	3	1884
400	1297	-1265	7.37	16	2562
500	1682	-1610	9.22	36	3292
600	2057	-1939	11.06	59	3996
700	2441	-2263	12.90	89	4704
800	2848	-2599	14.75	125	5447
900	3277	-2953	16.59	162	6230
1000	3673	-3284	18.43	195	6957
1100	4112	-3646	20.27	233	7758

Table 5.8: Test results for ESST-CO specimens

Specimen	Ult. Load (kN)	Strain near to failure		Shear modulus, (GPa)	Shear strength, τ (MPa)	Shear strain, γ ($\mu\varepsilon$)	Time to failure (sec)
		-45°	45°				
ESST-C01	1.391	-3646	4112	3.14	28.78	7758	68.00
ESST-C02	1.602	-4950	4688	3.19	32.36	9638	67.00
ESST-C03	1.298	-5048	4676	3.05	27.14	9724	61.00
ESST-C04	1.290	-4540	4071	2.85	26.32	8611	59.00
ESST-C05	1.550	-5615	5028	2.61	31.58	10643	77.00
Average	1.43			2.97 (0.24)	29.24 (2.66)	9275	66.40

Note: The value listed in bracket represent the standard deviation.

From Table 5.8, it can be seen that the highest ultimate failure load for the controlled sample was 1.60 kN and the lowest was 1.29 kN. For this controlled sample, the average ultimate failure load was 1.43 kN. The average shear modulus

and the shear strength are 2.97 GPa (i.e. about 8% of specimens data value deviated from their average value) and 29.24 MPa (i.e. about 9% of specimens data value deviated from their average value), respectively. As compared to the manufacturer's specifications, the shear strength for Selfix Carbofibe adhesive was higher than 18 MPa (i.e. under single lap shear test method). The value of shear strength obtained from the Arcan test method for controlled sample was 62.44% higher than the minimum manufacturer's quoted value. The average time taken to fail for most of the specimens was about 66.4 seconds while the total average of shear strain was 9275 $\mu\epsilon$.

The shear stress and shear strain data in Table 5.7 were used in plotting the shear stress versus shear strain curve as shown in Fig. 5.26. The stress-strain curve shows that strain on each specimen was linearly propagated. The difference of recorded strain values between strain gauges +45° and -45° was about 7%, which shows that any loading misalignment from as little as 1° from normal may cause a 6% difference in shear property [77].

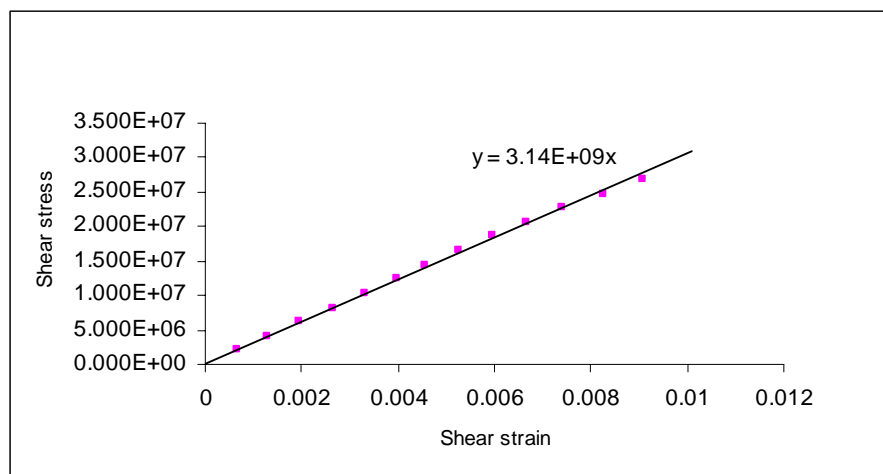


Fig. 5.26: Shear stress-strain curve for ESST-C01

During testing, it could be observed that the ESST specimen linearly gained shear loads from the start until up to failure, and had shown brittle type of failure mode as shown in Fig. 5.27. The fracture mechanism of the epoxy appeared to be initiated from the notch roots of the specimen. This fracture surfaces were found at 45° to the loading axis, which was the direction of the tensile principal stress

corresponding to the state of the pure shear as shown in Fig. 5.28. Such failure mechanism was also found in the Iosipescu test method on vinyl ester specimen conducted by Sullivan *et al.* [64], and Arcan test method conducted by Yen *et al.* on Plexiglas specimen [63].

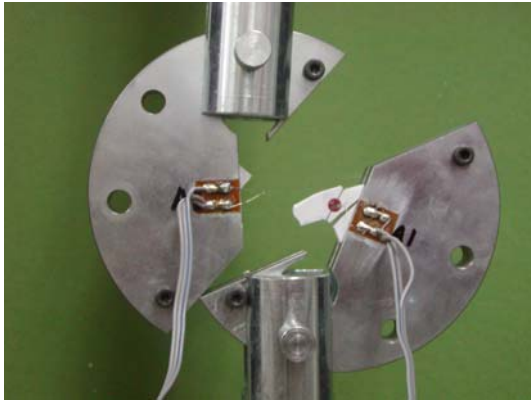


Fig. 5.27: Specimen ESST just after failure

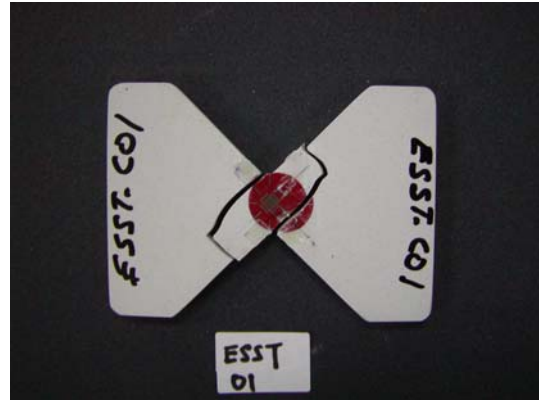


Fig. 5.28: Brittle failure of ESST-C01 occurred at $\pm 45^\circ$

5.8.3 Experimental Results for Laboratory Exposure (ESLT-LB)

For laboratory exposure condition, only four (4) specimens in the sample were tested because specimen ESLT-LB05 has broken during experimentation. In this sample, all test specimens, ESLT-LB01 to ESLT-LB04 have shown brittle characteristics of failure. The raw data for ESLT-LB01 specimen are shown in Table 5.9 and the complete test data for the laboratory sample, which was calculated from previously stated equations, are shown in Table 5.10.

Table 5.9: Experimental data for ESLT-LB01

Load (N)	Principal strain ε_{+45} ($\mu\varepsilon$)	Principal strain ε_{-45} ($\mu\varepsilon$)	Average shear stress τ_{ave} (MPa)	Average strain, ε_x ($\mu\varepsilon$)	Shear strain, γ ($\mu\varepsilon$)
100	399	-301	2.03	49	700
200	374	-656	4.06	-141	1030
300	1182	-1013	6.09	84.5	2195
400	1508	-1312	8.12	98	2820
500	1890	-1675	10.16	107.5	3565
600	2245	-2015	12.19	115	4260
700	2697	-2437	14.22	130	5134
800	3133	-2819	16.25	157	5952
900	3526	-3145	18.28	190.5	6671
1000	3996	-3512	20.32	242	7508

Table 5.10 Test results for ESLT-LB specimens

Specimen	Ult. Load (kN)	Strain near to failure		Shear modulus, (GPa)	Shear strength, τ (MPa)	Shear strain, γ ($\mu\varepsilon$)	Time to failure (sec)	Weight gain (%)
		-45°	45°					
ESLT-LB01	1.078	-3512	3996	2.76	21.89	7508	46.56	0.102
ESLT-LB02	1.017	-4006	4613	2.22	20.80	8619	44.97	0.093
ESLT-LB03	1.017	-3636	4193	2.53	19.79	7829	55.19	0.104
ESLT-LB04	1.195	-3739	4330	2.84	24.81	8069	53.54	0.118
Average	1.08			2.59 (0.28)	21.82 (2.17)	8006	50.07	0.104 (0.011)

Note: The value listed in bracket represent the standard deviation.

From Table 5.10, all specimens experienced weight gain when exposed to the laboratory condition. The average weight gain was about 0.1% and was suspected to be due to moisture absorption from the surroundings of controlled room, as the specimens experienced 75 to 90% relative humidity (RH) in 23 to 33°C room temperature during the six months of exposure period. The highest ultimate failure load in the sample was 1.195 kN and the lowest was 1.017 kN. For this laboratory sample, the average ultimate failure load was 1.08 kN. The average shear modulus and the shear strength were 2.59 GPa (i.e. about 11% of specimens data value deviated from their average value) and 21.82 MPa (i.e. about 10% of specimens data value deviated from their average value), respectively. These shear modulus and shear strength for laboratory exposure were 12.8 and 25.34% lower as compared to

the control sample. Average time taken to fail for most of the specimens was about 50.07 seconds while the total average of shear strain was 8006 $\mu\epsilon$.

The shear strain versus shear stress curve, as shown in Fig. 5.29, was then plotted to show the relation between them. It can be seen that the ESLT-LB specimens linearly gained shear loads from the start up to failure, but the curve was initially non-linear which might be due to slippage of specimen during the testing. However, this was negligible as it was too small.

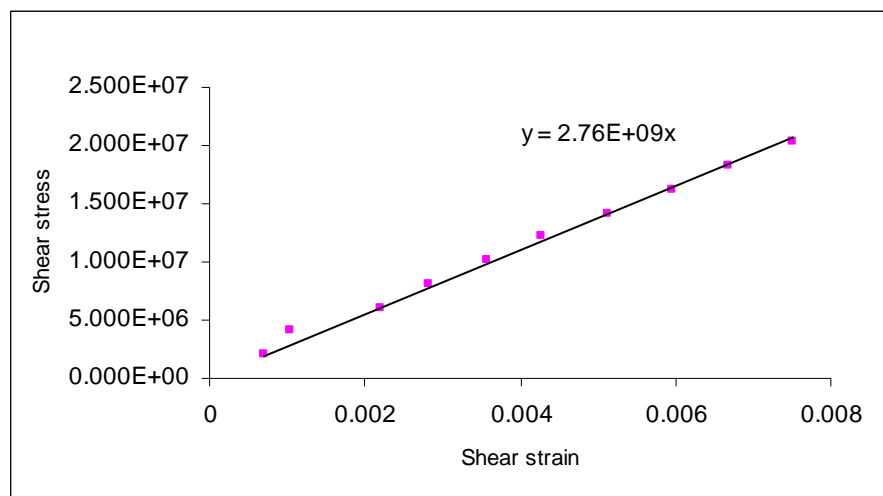


Fig. 5.29: Shear stress-strain curve for ESLT-LB01

From the stress-strain curve in Fig. 5.29, it can be noted that all specimens have perfectly failed in a brittle manner. The fracture surfaces of laboratory specimens were also found at almost 45° to the loading axis, which was the direction of the tensile principal stress corresponding to the state of the pure shear, as shown in Figs. 5.30 (a) and (b).



Fig. 5.30 (a): Specimen ESLT-LB01 just after failure

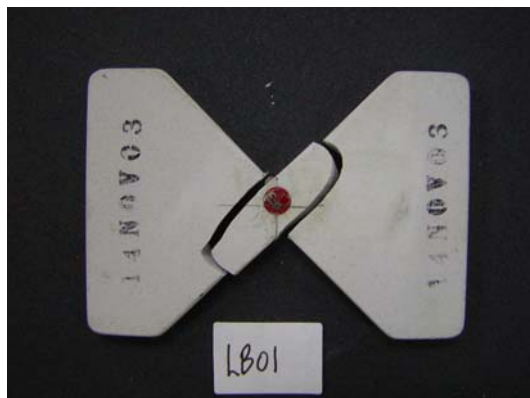


Fig. 5.30 (b): Brittle failure of ESLT-LB01 specimen

5.8.4 Experimental Results for Outdoor Exposure (ESLT-OD)

There are four (4) specimens that represented the outdoor sample (specimen ESLT-OD05 had broken during the experimentation period). All the specimens (ESLT-OD01 to ESLT-OD04) showed brittle characteristics up to failure. The raw data for ESLT-OD01 specimen are presented in Table 5.11, and the complete analysed data for the laboratory sample are shown in Table 5.12.

Table 5.11: Experimental data for ESLT-OD01

Load (N)	Principal strain ϵ_{+45} ($\mu\epsilon$)	Principal strain ϵ_{-45} ($\mu\epsilon$)	Average shear stress, τ_{ave} (MPa)	Average strain, ϵ_x ($\mu\epsilon$)	Shear strain, γ ($\mu\epsilon$)
100	257	-86	2.06	85.5	343
200	574	-303	4.13	135.5	877
300	955	-615	6.20	170	1570
400	1350	-949	8.26	200.5	2299
500	1729	-1280	1.03	224.5	3009
600	2576	-1992	1.24	292	4568
700	2987	-2327	1.44	330	5314
800	3489	-2715	1.65	387	6204
900	4109	-3145	1.86	482	7254

Table 5.12: Test results for ESLT-OD specimens

Specimen	Ult. Load (kN)	Strain near to failure		Shear modulus (GPa)	Shear strength, τ (MPa)	Shear strain, γ ($\mu\epsilon$)	Time to failure (sec)	Weight loss (%)
		-45°	45°					
ESLT-OD01	1.011	-3145	4109	2.76	20.89	7254	43.11	0.094
ESLT-OD02	1.097	-4594	3767	2.55	23.06	8361	50.47	0.097
ESLT-OD03	1.301	-4625	4683	2.66	26.15	9308	46.52	0.097
ESLT-OD04	1.243	-4542	4276	2.83	25.29	8818	43.23	0.104
Average	1.16			2.70 (0.12)	23.85 (2.36)	8435	45.83	0.098 (0.004)

Note: The value listed in bracket represent the standard deviation.

For OD sample, all specimens experienced weight loss (Table 5.12) which was highly suspected to be due to exposure to wet-dry condition (i.e. hot and rain) for the duration of six months. The average specimen weight reduction for ESLT-OD sample was about 0.1%. The yellowish effect could be clearly visualised with some dust forming on the specimen's surfaces.

The highest ultimate failure load for the sample was 1.30 kN and the lowest was 1.01 kN. For outdoor sample, the average ultimate failure load was 1.16 kN. The average shear modulus and shear strength was 2.70 GPa (i.e. about 4% of specimens data value deviated from their average value) and 23.85 MPa (i.e. about 10% of specimens data value deviated from their average value), respectively. Shear modulus and shear strength for the outdoor sample were 18.4% and 9.09% lower when compared to controlled sample (as previously stated). The average time to failure was about 45.83 seconds. The highest shear strain was 9308 $\mu\epsilon$, i.e. for specimen ESLT-OD03, and the average shear strain value for OD sample was 8435 $\mu\epsilon$.

During the test, it could be seen that the ESLT-OD specimens linearly gained shear loads from the start up to failure. However, for the outdoor exposure sample ESLT-OD, the graph was not perfectly linear, which might be due to high brittleness, suspected from porosities that formed at the significant section cross section. Apart from that, the specimen's cross sectional area was the lowest compared to other exposure conditions. The shear stress and shear strain data in Table 5.11 were then used to plot the strain-shear stress curve as shown in Fig. 5.31.

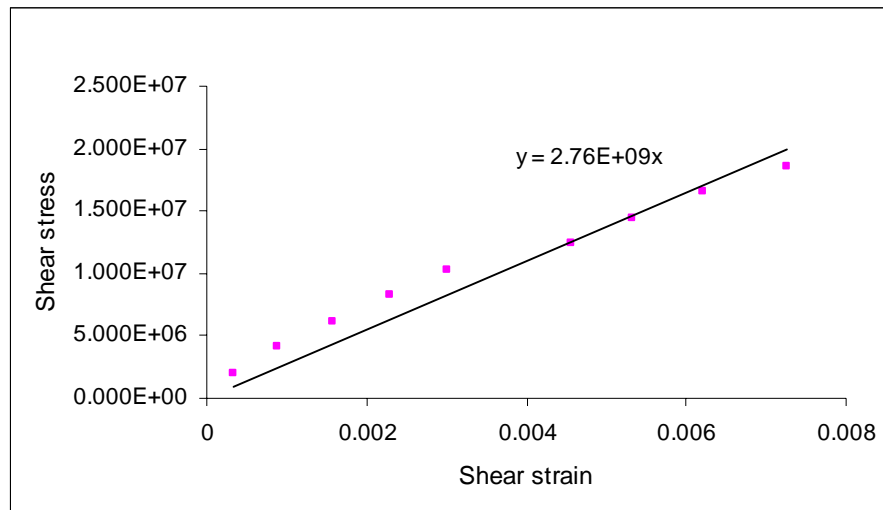


Fig. 5.31: Shear stress-strain curve for ESLT-OD01

From Fig. 5.31, the plotted stress-strain curve is not perfectly linear, which might be due to the yellowish effect resulting from the oxidation process which increased the level of material brittleness, or might be due to the creation of micro-cracks resulting from the exposure to hot/wet environment. The yellowish effect could break the polymer chain which finally led the specimen to fail at a lower than expected load. However, the strain-shear stress curve shown in Fig. 5.29 has verified that a state of pure shear was present during the testing. Other than that, porosities were suspected to occur at the significant section (AB) that caused cracks to initiate faster from the notch roots of the specimen, which was 45° to the direction of the tensile principal stress (i.e. loading axis) as shown in Fig. 5.32 (a) and (b).



Fig. 5.32 (a): Specimen ESLT-OD01 just after failure

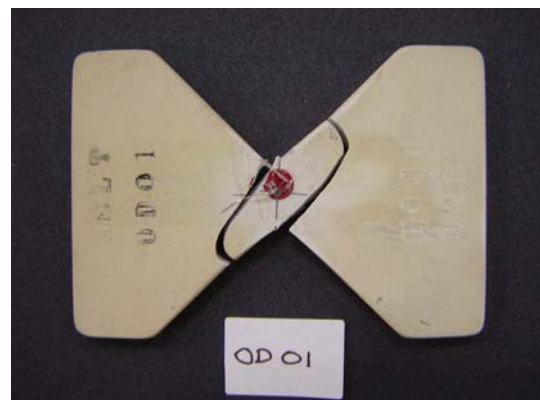


Fig. 5.32 (b): Brittle failure of ESLT-OD01 specimen

5.8.5 Experimental Results for Plain Water Wet-Dry Exposure (ESLT-PW)

For plain water wet-dry exposure condition, five (5) specimens have been tested. All specimens have shown brittle characteristics of failure. The raw data for ESLT-PW01 specimen are presented in Table 5.13 and the complete analysed test data for the plain water (w/d) specimens are shown in Table 5.14.

Table 5.13: Experimental data for ESLT-PW01

Load (N)	Principal strain ε_{+45} ($\mu\varepsilon$)	Principal strain ε_{-45} ($\mu\varepsilon$)	Average shear stress τ_{ave} (MPa)	Average strain, ε_x ($\mu\varepsilon$)	Shear strain, γ ($\mu\varepsilon$)
100	534	-206	2.09	164	740
200	850	-405	4.19	222.5	1255
300	1124	-563	6.28	280.5	1687
400	1408	-725	8.38	341.5	2133
500	1742	-953	1.04	394.5	2695
600	2103	-1231	1.25	436	3334
700	2467	-1523	1.46	472	3990
800	2058	-1844	1.67	107	3902
900	3245	-2132	1.88	556.5	5377

Table 5.14: Test results for ESLT-PW specimens

Specimen	Ult. Load (kN)	Strain near to failure		Shear modulus, (GPa)	Shear strength, τ (MPa)	Shear strain, γ ($\mu\varepsilon$)	Time to failure (sec)	Weight gain (%)
		-45°	45°					
ESLT-PW01	1.011	-2132	3245	3.76	21.20	5377	52.64	0.272
ESLT-PW02	0.827	-3715	4297	2.04	17.05	8012	46.01	0.246
ESLT-PW03	0.895	-3978	4396	1.97	18.44	8374	48.59	0.267
ESLT-PW04	1.058	-3984	4737	2.42	21.59	8721	47.23	0.268
ESLT-PW05	1.100	-3081	3564	2.99	21.14	6645	49.48	0.168
Average	0.98			2.64 (0.75)	19.88 (2.02)	7426	48.79	0.244 (0.044)

Note: The value listed in bracket represent the standard deviation.

According to Table 5.14, there was an increment in weight for all specimens as they experienced wet/dry cycles for the duration of sixth months in plain water. The average weight gain for plain water exposure sample was 0.24%. The highest ultimate failure load in the sample was 1.10 kN and the lowest was 0.83 kN. For this sample their average ultimate failure load was 0.98 kN. The average shear modulus

and shear strength were 2.64 GPa (i.e. about 3% of specimens data value deviated from their average value) and 19.88 MPa (i.e. about 10% of specimens data value deviated from their average value), respectively. The shear modulus and shear strength for plain water sample was 11.10% and 32.01% lower as compared to the control sample. The average time to failure for most of the specimens was about 48.79 seconds, while the highest shear strain was 8721 $\mu\epsilon$, which occurred on specimen ESLT-PW04.

The shear strain versus shear stress curve, as shown in Fig. 5.33 was then plotted to show the relation between shear stress and shear strain. It can be seen that the ESLT-PW specimens linearly gained shear loads from the start up to failure, but the curve was not perfectly linear at the end of the failure, suspected from the formation of micro-porosities at the cross-section or epoxy chemical degradation through moisture diffusion.

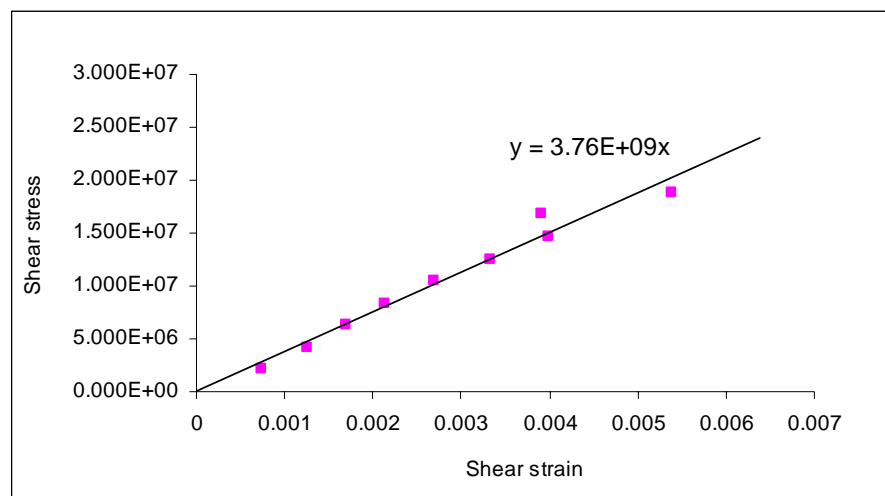


Fig. 5.33: Shear stress-strain curve for ESLT-PW01

All the specimens in the plain water wet-dry exposure have shown brittle failure characteristics under load. This fracture surfaces were found at 45° to the loading axis, which was the direction of the tensile principal stress corresponding to the state of the pure shear, as shown in Fig. 5.34 (a) and (b).



Fig. 5.34 (a): Specimen ESLT-PW01 just after failure

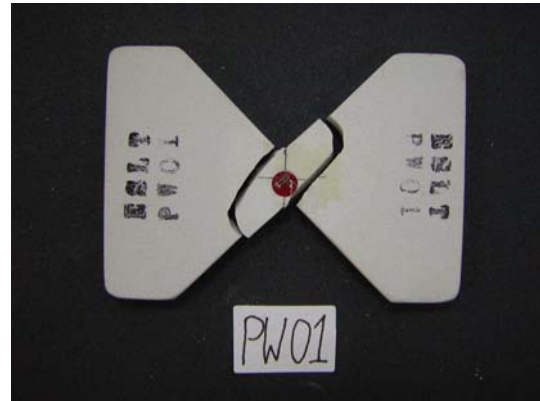


Fig. 5.34 (b): Brittle failure of ESST-PW01

5.8.6 Experimental Results for Salt Water Wet-Dry Exposure (ESLT-SW)

There were five (5) specimens in the sample of salt water wet-dry exposure condition. All specimens, ESLT-SW01 to ESLT-SW05 have shown brittle characteristics of failure. The raw data for ESLT-SW01 specimen are shown in Table 5.15, and the complete test data for the plain water specimens are shown in Table 5.16.

Table 5.15: Experimental data for ESLT-SW01

Load (N)	Principal strain ϵ_{+45} ($\mu\epsilon$)	Principal strain ϵ_{-45} ($\mu\epsilon$)	Average shear stress τ_{ave} (MPa)	Average strain, ϵ_x ($\mu\epsilon$)	Shear strain, γ ($\mu\epsilon$)
100	358	-312	1.99	23	670
200	672	-607	3.99	32.5	1279
300	977	-932	5.98	22.5	1909
400	1267	-1235	7.98	16	2502
500	1603	-1573	9.98	15	3176
600	1938	-1893	1.19	22.5	3831
700	2301	-2234	1.39	33.5	4535
800	2660	-2564	1.59	48	5224
900	3046	-2914	1.79	66	5960
1000	3537	-3338	1.99	99.5	6875
1100	4221	-3827	2.19	197	8048

Table 5.16: Test results for ESLT-SW specimens

Specimen	Ult. Load (kN)	Strain near to failure		Shear modulus, (GPa)	Shear strength τ (MPa)	Shear strain, γ ($\mu\epsilon$)	Time to failure (sec)	Weight gain (%)
		-45°	45°					
ESLT-SW01	1.119	-3827	4221	2.94	22.34	8048	45.00	2.735
ESLT-SW02	0.871	-3841	4389	2.04	18.19	8230	40.27	2.778
ESLT-SW03	1.091	-3550	4038	2.77	22.33	7588	44.10	2.709
ESLT-SW04	0.949	-4293	4700	2.11	19.78	8993	55.85	2.773
ESLT-SW05	1.289	-3566	4961	2.86	24.62	8527	54.04	2.371
Average	1.06			2.54 (0.43)	21.45 (2.50)	8277	47.85	2.673 (0.171)

Note: The value listed in bracket represent the standard deviation

By referring to the test results as listed in Table 5.16, the average weight gain for all specimens was of about 2.67%. This weight gain occurred due to absorption process during the six months to salt water exposure. The highest ultimate failure load in the sample was 1.289 kN and the lowest was 0.871 kN. The average ultimate failure load was 1.06 kN.

For the shear properties, the average shear modulus and shear strength were 2.54 GPa (i.e. about 17% of specimens data value deviated from their average value) and 21.45 MPa (i.e. about 12% of specimens data value deviated from their average value), respectively. The average values of shear modulus and shear strength obtained from the salt water exposure condition were 14.48% and 33.05% lower compared to the control sample. The average time to failure for most of the specimens was about 47.85 seconds while the average of shear strain for the sample was 8277 $\mu\epsilon$.

The shear stress-strain curve for ESLT-SW01 is shown in Fig. 5.35. The stress strain curve shows a linear relationship between shear stress and shear strain, thus the shear modulus was obtained from the curve gradient. During testing, it could be observed that the ESST-SW01 specimen linearly gained shear loads from the start up to failure, and has shown a brittle type failure.

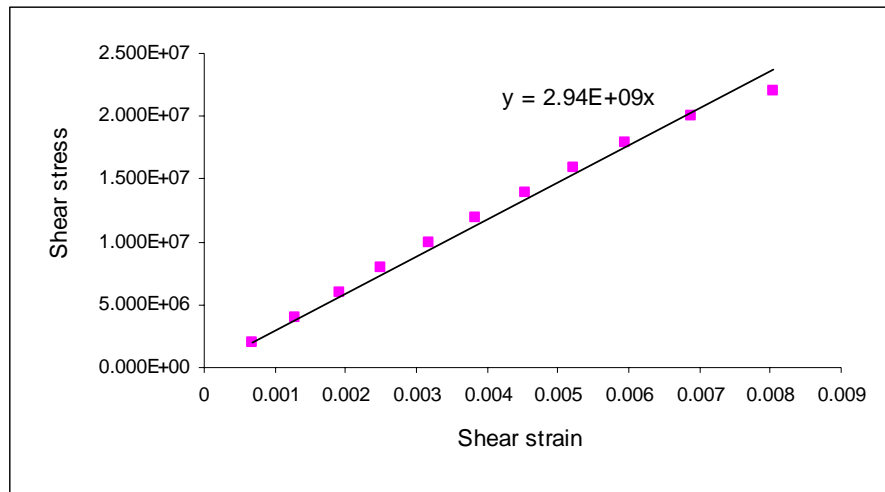


Fig. 5.35: Shear stress-strain curve for ESLT-SW01

The fracture surfaces for salt water specimens were also found at almost 45° to the loading axis, which was the direction of the tensile principal stress corresponding to the state of the pure shear, as shown in Fig. 5.36 (a) and (b).

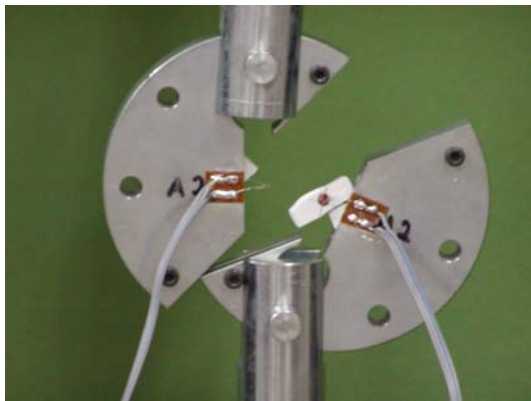


Fig. 5.36 (a): Specimen ESLT-SW01 just after failure

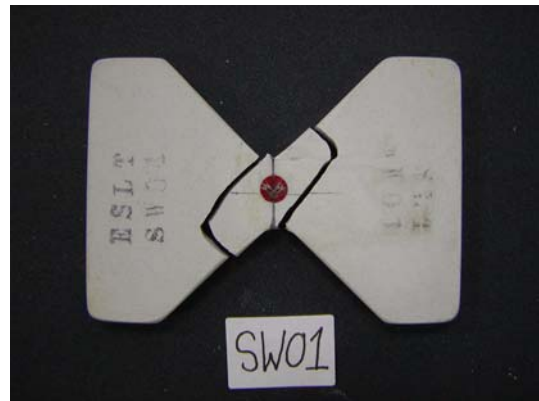


Fig. 5.36 (b): Brittle failure of ESLT-SW01

5.8.7 Overall Results Discussion

From the overall results a comparison between shear strength and their respective weight gain and reduction factors were established as listed in Table 5.17.

Table 5.17: Overall properties of Selfix Carbofibe adhesive exposure group of specimens

Exposure condition	Shear strength, τ (MPa)	Shear modulus, G (GPa)	Weight gain (%)	Weight loss (%)	Time to failure (s)
Controlled	29.24 (9%)	2.97 (8%)	-	-	66.4
Laboratory	21.82 (10%)	2.59 (11%)	0.11	-	50.07
Outdoor	23.85 (10%)	2.70 (4%)	-	0.10	45.83
Plain Water	19.88 (10%)	2.64 (3%)	0.25	-	48.79
Salt Water	21.45 (12%)	2.54 (17%)	2.67	-	47.85

Note: The values listed in bracket represent the percentage of data value deviated from their average value.

From Table 5.17, it shows that the ESLT-OD sample had the highest shear strength which was 23.85 MPa, followed by ESLT-LB, 21.82 MPa, ESLT-SW, 21.45 MPa; and finally the ESLT-PW, 19.88 MPa. Based on the results, it can be said that the specimens' shear strength was reduced effecting from the exposure to wet/dry cycles in plain and salt water. The moisture diffusion mechanism could be seen through the 0.25 to 2.67% in specimen's weight gain.

The chemical chain of the epoxy might be weakened as the water penetrated through diffusion mechanism. Another factor that influenced and affected the shear strength was the oxidation process for ESLT-OD specimens, as the weight was reduced by about 0.10% by means of yellowish effect on specimens as they were exposed to wet/dry outdoor condition. The epoxy shear strength versus exposure conditions is shown in Fig. 5.37. The shear strength for ESLT-LB, ESLT-OD, ESLT-PW and ESLT-SW were lower than the control sample, ESST-CO. ESLT-PW sample had the lowest shear strength value, which was 32% lower than the controlled sample, followed by ESLT-SW, 26.6%, ESLT-LB, 25.4%; and finally the ESLT-OD, 18.4%.

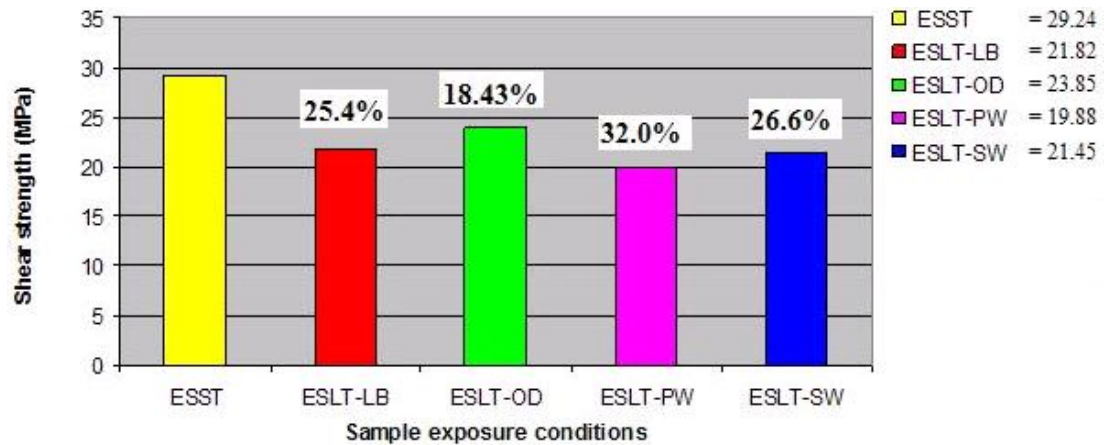


Fig. 5.37: Shear strength versus exposure condition for all test samples

The epoxy shear modulus versus exposure conditions is shown in Fig.5.38. The shear modulus for ESLT-LB, ESLT-OD, ESLT-PW and ESLT-SW were also lower than the controlled sample, ESST-CO. ESLT-SW sample had the lowest shear modulus value, which was 14.5% lower than the control sample, followed by ESLT-LB (12.8%), ESLT-PW (25.4%) and finally the ESLT-OD (9.0%).

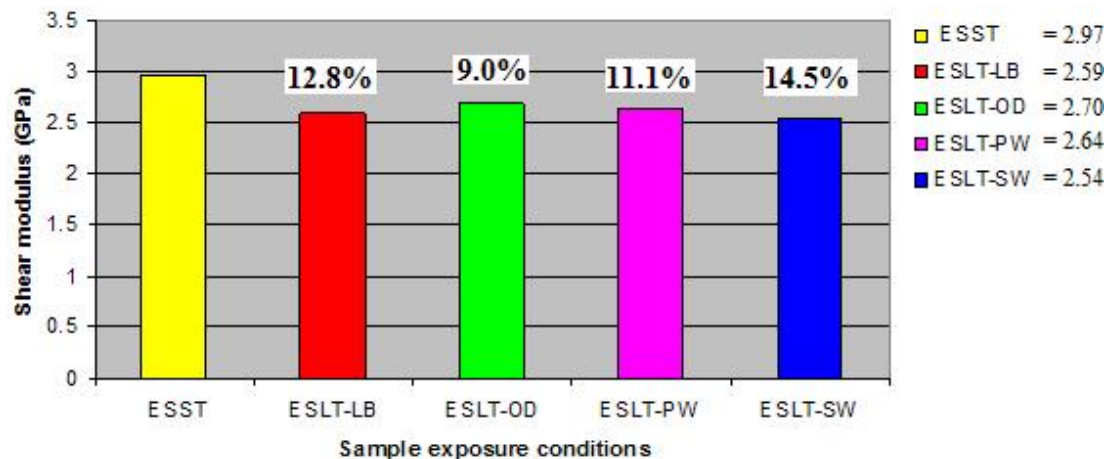


Fig. 5.38: Shear Modulus versus sample exposure conditions for all test samples

From the theory, it was assumed that the material was homogeneous and isotropic. Unfortunately, this condition did not exist in Selfix Carbofibe adhesive epoxy due to the formation of micro-porosity. The testing method and procedure also played important roles in obtaining accurate test results. As an example, the bonding of the specimen to the Arcan fixture and the test rig alignment also provided a significant effect to the experimental results [63]. Each manufacturer has its own

testing specification, which may differ from each other. This is very much dependent on the manufacturer's definition and procedure of testing. More importantly, their testing method refers directly on the materials actual application.

5.9 FESEM Microstructure Analysis on Failure Specimens

Besides the discussion on the shear strength and shear modulus of the specimens, microstructure analysis is also an important subject to focus on in order to obtain the factors that may affect the strength of epoxy adhesive due to tropical exposure conditions. An investigation was made to find out the influences of the environment conditions (tropical conditions) on the epoxy structural system. For that purpose, the fracture parts and specimens surfaces were analysed by using Field-emission Scanning Electron Microscope (FESEM).

5.9.1 Chemical Elements in Selfix Carbofibe Adhesive

After the samples have been exposed to the designated conditions, selected specimens underwent scanning process by using the FESEM microscope. The main objective was to determine the changes of base elements in each sample. The base elements for each sample are presented in Table 5.18.

Table 5.18: Chemical elements weight percentage for Selfix Carbofibe adhesive after exposure

Exposure Condition	Specimen	Elements Weight (%)					
		O	C	Si	Ti	Mg	Cl
Controlled	ESST-C02	35.66	49.30	12.35	1.46	0.29	0.95
Laboratory	ESLT-LB01	34.35	47.97	14.54	2.22	0.19	0.73
Outdoor	ESLT-OD03	35.01	50.94	11.30	1.75	0.30	0.70
Plain Water	ESLT-PW05	34.35	52.14	11.02	1.84	0.08	0.57
Salt Water	ESLT-SW03	35.83	49.97	11.76	1.52	0.22	0.71

From Table 5.18, an assumption has been made that the shear strength and shear modulus of each exposure conditions depended on the contents of Silicon, Magnesium, (Mg), Titanium, (Ti), and Carbon, (C). Silicon was the main filler in the epoxy system which was added to enhance the bond properties. However, the composition of silicon in each specimen was distributed unevenly due their geometrical non-uniformity. The highest magnesium contents was in ESLT-OD03, followed by ESLT-C02, ESLT-SW03, and finally ESLT-PW05. Other elements contents such as oxide, chlorine and silicone in specimens did not differ much for each exposure condition.

5.9.2 Analysis on Fracture Part Cross-section

All the Selfix Carbofibe adhesive experimentation specimens failed in brittle form at failure load. One of the factors that influenced the accuracy and reliability of the test data is the formation of micro-porosity, as shown in Fig. 5.39 (a). Among the factors that lead to the formation of porosity were most probably due to the mixing speed and materials composition geometrical effects (not uniform in sizes). If the formation of micro-porosity were high in volume or area, the failure due to tensile was highly dominant and the specimen failed at a load lower than expected.

Every specimen that represented their respective sample was scanned of their fracture part cross-section at three different locations. The image was scanned by using 200 magnification scale factor (The porosity size was measured by using scale of 13 mm = 10 μ m).

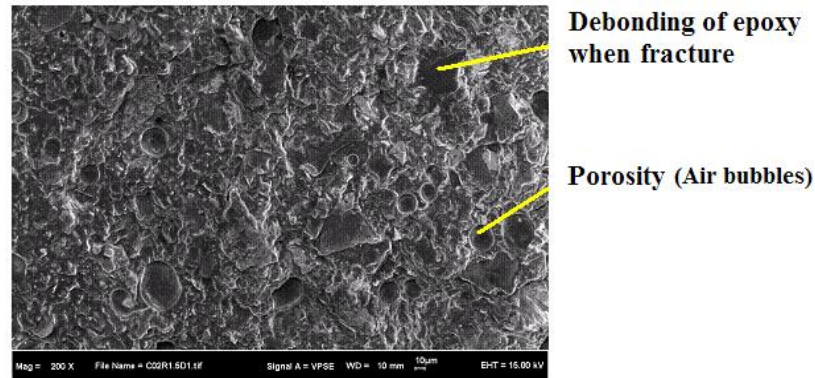


Fig. 5.39 (a): Fracture cross-section surface of ESST-CO

The results have also shown that the porosities were formed for all specimens (i.e. ESLT-LB, ESLT-OD, ESLT-PW and ESLT-SW) as shown in Fig. 5.39 (b) to (e). The micro-porosity size measured for ESST-CO specimen was about $80.25\ \mu\text{m}$, as shown in Fig. 5.40. As previously stated, the micro-porosity was the critical factor that accelerated the failure for each respective specimen. From these figures, it is shown that the micro-porosities sizes were totally uneven for each specimen.

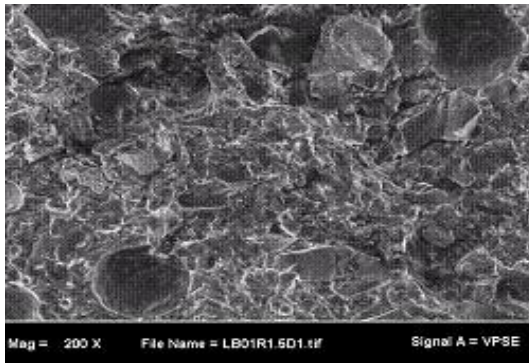


Fig. 5.39 (b): Micro-porosities in ESLT-LB

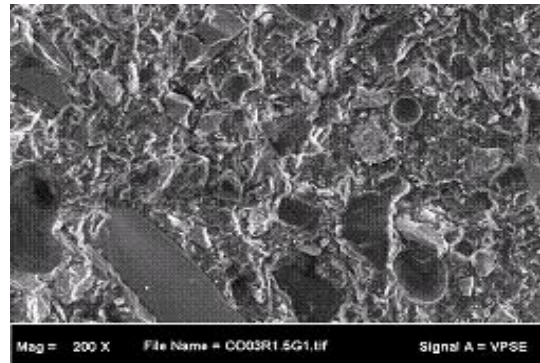


Fig. 5.39 (c): Micro-porosities in ESLT-OD

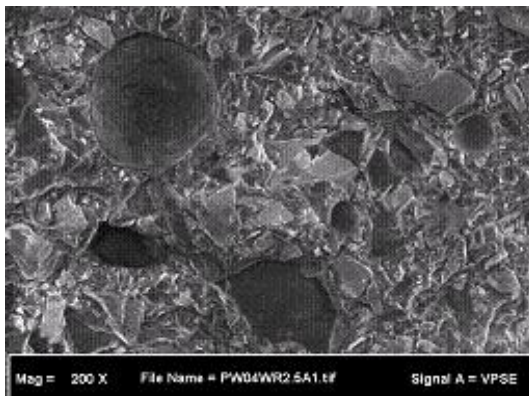


Fig. 5.39 (d): Micro-porosities in ESLT-PW

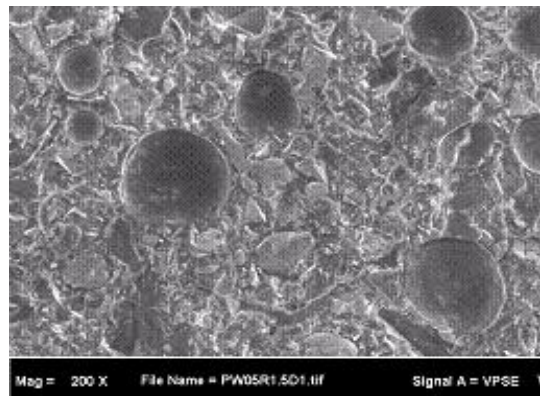


Fig. 5.39 (e): Micro-porosities in ESLT-SW

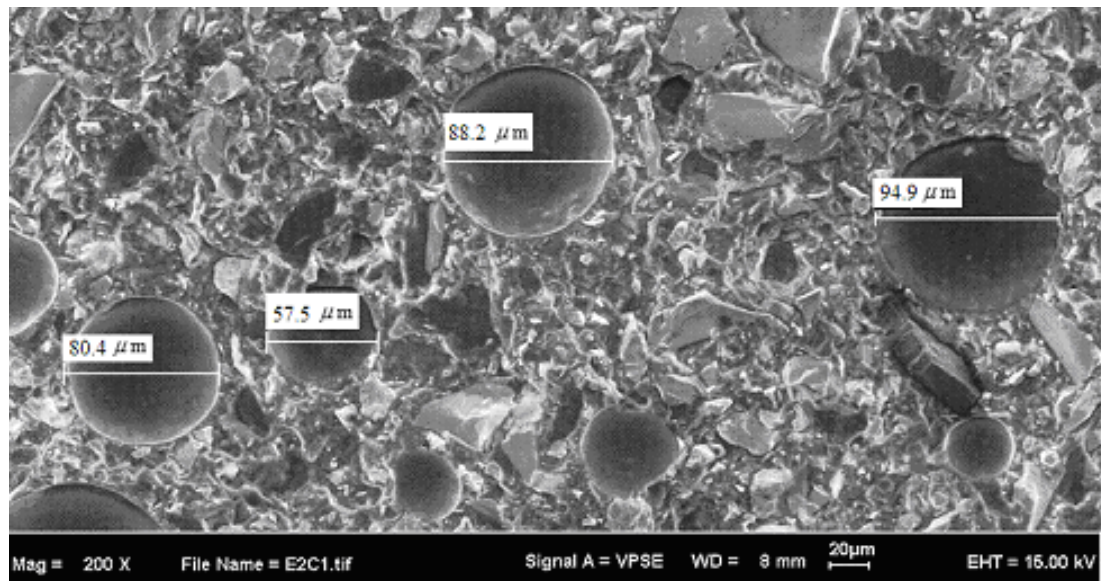


Fig. 5.40: The formation of micro-porosities size in ESST-CO

5.9.3 Analysis on Fracture Part Surface

It is very important to study the effect of exposure conditions on epoxy through microstructure analysis in order to gain more information to support the analytical test data. The microstructure analysis results using FESEM for all selected exposure specimen can be referred to in Fig. 5.41 to Fig. 5.45.

Fig. 5.41 shows the standard texture of the epoxy's top surface that experienced no exposure effects (i.e. control specimen). The figure shows perfect bonding between epoxy matrix and silicon based filler that was used to enhance the mechanical properties of the epoxy system. By referring to Fig. 5.42, it is clear that the ESLT-LB material texture experienced environmental effect due to the surrounding air that contained high moisture level in the laboratory. The significant effect of the six months exposure period on the ESLT-OD specimen was the formation of crack line that was probably caused by oxidation process, as shown in Fig. 5.43. The specimen also experienced unpredictable chemical effects due to the outdoor weathering or climate changes such as temperature fluctuation, presence of high humidity level, reaction to mineral rain content [31], ultraviolet radiation and etc. The metal elements composed in the epoxy system (Table 5.18) also tendency to

react with oxygen (O_2) in the air and formed metal oxide such as MgO and TiO_3 (in form of dust) [89]. The effect has reduced the weight of the specimen as previously reported in section 5.8.7.

The effect of plain water on ESLT-PW top surface can be seen in Fig 5.44. There was a sign of erosion and cracking occurring on the material surface. Generally, epoxy adhesive is prone to water absorption because they possess polar sites that attract water molecules through diffusion mechanism. Water molecules are typically hydrogen bonded to hydrophilic groups of cured epoxy, mainly hydroxyl and amine groups [90]. The absorption of water has greatly influenced the strength of the epoxy structure (Table 5.14). Water might have penetrated the epoxy system by diffusion or capillary action through cracks or porosity. The water molecules that entered into the epoxy material bond with the polymer through hydrogen bonding. By this mechanism, the water was able to disrupt the inter chain Van der Waals forces inside the network producing an increased of segmental mobility [91]. This hydrolysis of the bisphenol-A epoxy by water absorption is a form of chemical degradation of the matrix.

The effect of saltwater exposure condition for ESLT-SW specimen can be seen in Fig. 5.45, where the formation of salt (NaCl) that adhered to the specimen surface could be observed. This might be caused by a volume of saltwater that has already saturated in the specimen due to absorption process. The specimen has experienced the highest weight gain which was about 2.67% (Table 5.16). The density of the saltwater that is higher than plain water has caused more absorption into the specimen. The chemical reaction formed between NaCl ions and epoxy polymer system was a possibility that the shear properties of the specimen has reduced. The epoxy that initially consisted of siklo bonds was reduced to single bond due to the chemical reaction between Na^+ Cl^- and epoxy. It is known that, the strength of a single bond is actually weaker than siklo bond.

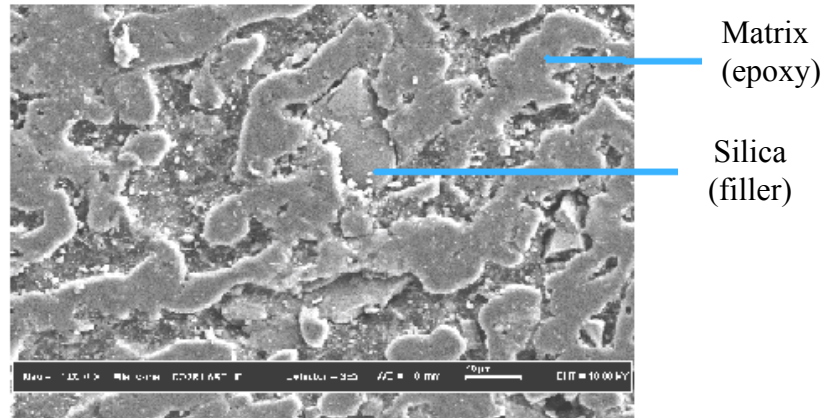


Fig. 5.41: ESST-C0 surface texture

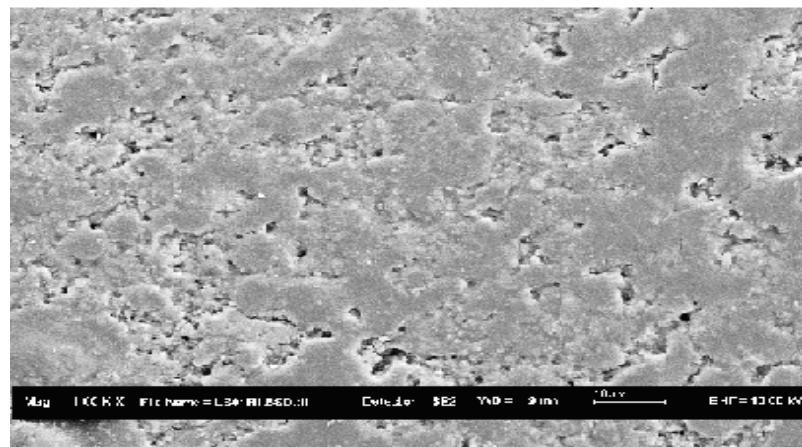


Fig. 5.42: ESLT-LB surface texture exposed to laboratory condition

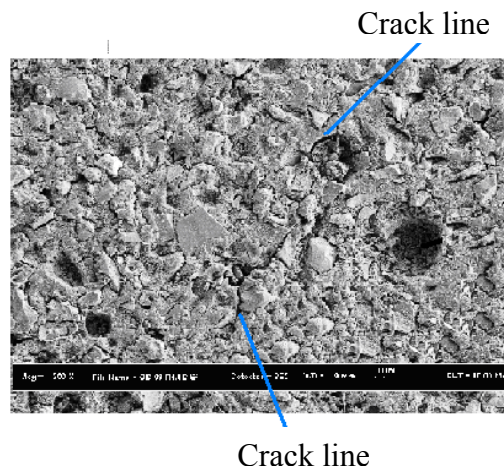


Fig. 5.43: ESLT-OD surface texture exposed to outdoor condition

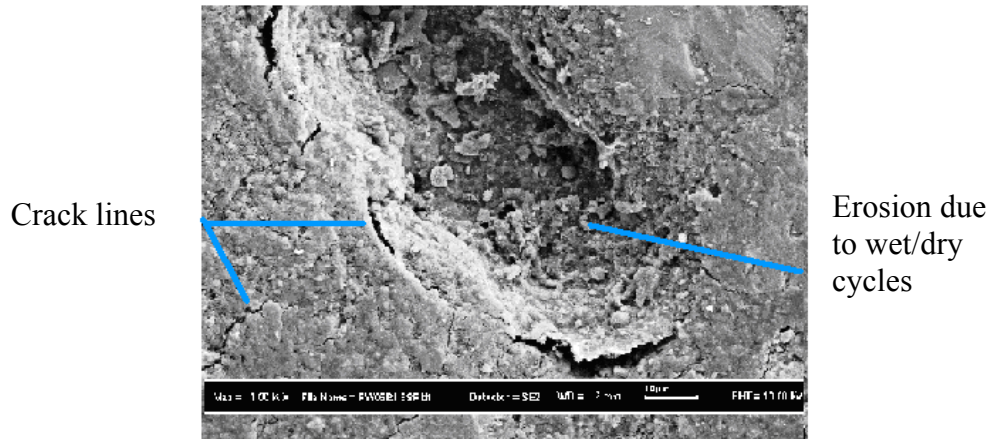


Fig. 5.44: ESLT-PW surface texture exposed to plain water (wet/dry) condition

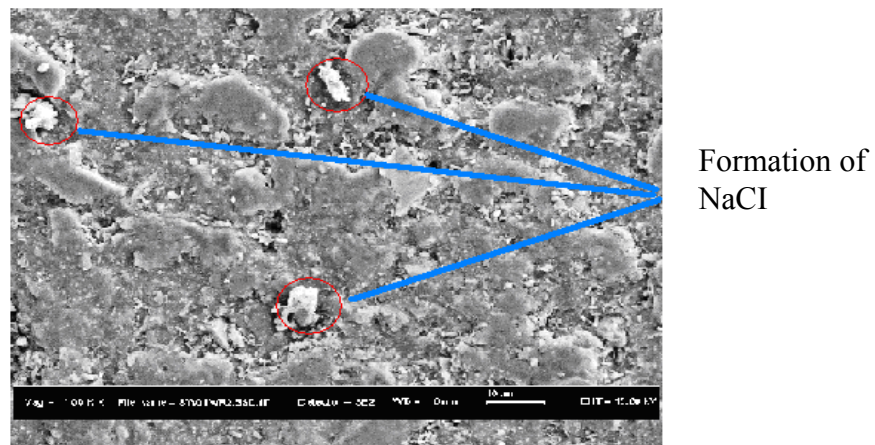


Fig. 5.45: ESLT-SW surface texture exposed to salt water (wet/dry) condition

5.10 Conclusions

The major conclusions that can be made from this study programme are summarised as follows;

- i. The study objective to determine the epoxy shear property (i.e. strength and modulus) using the Arcan test fixture was achieved. The significant section of the butterfly specimen has proven that the Arcan test method was reliable, as the shear stress and strain relationship was linearly propagated. The results also show that both strain directions were not

perfectly symmetrical for some of the specimens, resulting from micro-porosity effect. The overall results can be accepted as the average strain difference was only about 7%.

- ii. The formation of micro-porosity during casting process was difficult to be eliminated due to the geometrical effect of epoxy composition materials that led to air entrapment and finally reduced the epoxy cross-sectional area of the significant section. The effect was also a factor that accelerated the moisture diffusion process into the epoxy system.
- iii. All specimens failed in brittle form. The experimentation and load test results show that the exposure conditions had influenced the shear strength and modulus of the epoxy system, especially for those exposed to plain and salt water conditions. It can also be concluded that the saltwater exposure condition (wet/dry) had produced significantly varied shear modulus data (i.e. with 17% of the specimens value deviated from their average value). This shows that exposure to saltwater condition was among the most aggressive ones.